Comput. Methods Appl. Mech. Engrg. 198 (2009) 2039–2051

Contents lists available at ScienceDirect

Comput. Methods Appl. Mech. Engrg.

journal homepage: www.elsevier.com/locate/cma

# Mechanistic modeling of swarms

T.I. Zohdi *

*Department of Mechanical Engineering, University of California, Berkeley, CA 94720-1740, USA*

ARTICLE INFO

*Article history:*
Received 19 February 2008
Received in revised form 7 October 2008
Accepted 31 December 2008
Available online 14 January 2009

*Keywords:*
Swarms
Modeling
Simulation

ABSTRACT

In this work, we provide an introduction to an emerging field which has recently received considerable attention, namely the analysis and modeling of *swarms*. In a very general sense, the term *swarm* is usually meant to signify a group of objects (agents) that interact with one another and have a collective goal. Point-mass, particulate-like models are frequently used to simulate the behavior of groups comprised of individual units whose interaction are represented by inter-particle forces. The interaction "forces" can represent, for example in the case of Unmanned Airborne Vehicles (UAVs), motorized propulsion arising from inter-vehicle communication and then actuation resulting in thrust. For a swarm member, these forces have two main components, attraction and repulsion, with the fellow swarm members and the surrounding environment. This work develops and investigates (1) basic models of such systems, (2) properties of swarm models and (3) numerical algorithms, in particular temporally adaptive methods, for swarm-like systems.



## 1. Introduction

It has long been recognized that interactive cooperative behavior within biological groups or "swarms" is advantageous in avoiding predators or, vice versa, in capturing prey. For example, one of the primary advantages of a swarm-like decentralized decision making structure is that there is no leader and thus the vulnerability of the swarm is substantially reduced. Furthermore, the decision making is relatively simple and rapid for each individual, however, the aggregate behavior of the swarm can be quite sophisticated.

The modeling of swarm-like behavior has biological research origins, dating back at least to Breder [14]. It is commonly accepted that a central characteristic of swarm-like behavior is the tradeoff between long-range interaction and short-range repulsion between individuals. Models describing clouds or swarms of particles, where their interaction is constructed from attractive and repulsive forces, dependent on the relative distance between individuals, are commonplace. For reviews, see Gazi and Passino [29], Bender and Fenton [8] or Kennedy and Eberhart [59]. The field is quite large and encompasses a wide variety of applications, for example, the behavior flocks of birds, schools of fish, flows of traffic and crowds of human beings, to name a few. Loosely speaking, swarm analyses are concerned with the complex aggregate behavior of groups of simple members, which frequently are treated as particles (for example in Zohdi [87]).

A central objective of the present work is to provide basic mechanistic models, and numerical solution strategies for the direct simulation of the motion of swarms that can be achieved within a relatively standard computing equipment. Although the approach taken in the present work is based on mechanical force interaction, it is important to mention that there exist a large number of what one can term as "rule-driven" swarms, whereby interaction is not governed by the principles of mechanics but by proximal instructions such as: "if fellow swarm member gets close to me, attempt to retreat as far as possible" or "follow the leader", or "stay in clusters", etc. Many species, such as ant colonies [12], exhibit foraging-type behavior, in addition to the trail-laying-trail-following mechanism for finding food sources. During the search for food, they deposit a chemical substance, called *pheromone*, which decays over time. Fellow foragers (swarm members) detect and follow paths with a high pheromone concentration, i.e. where the food source is highly concentrated. Although this type of model can be useful in some applications, it will not be discussed in this work. Recent broad overviews of the field can be found in Kennedy and Eberhart [59] and Bonabeau et al. [11]. For instance, Dorigo et al. [24] presented an optimization algorithm based on the foraging behavior of ants which basically used a computer adaptation of the pheromone trail-laying-trail-following method to mimic the behavior of ants to allow the "software ants" to solve combinatorial problems such as the travelling salesman problem.[1] Bonabeau et al. [12] presented several such optimization algorithms, each one influenced by another feature of biological swarms. There are numerous other models in this direction to develop optimization techniques [12,59], businesses planning [13], tele-

* Tel.: +1 510 642 9172; fax: +1 510 642 6163.
*E-mail address:* zohdi@newton.berkeley.edu

[1] Finding the least expensive route for traveling to a number of given locations, given the costs for each connection route.

0045-7825/$ - see front matter © 2009 Elsevier B.V. All rights reserved.
doi:10.1016/j.cma.2008.12.029

communication network design [12], mobile sensor networks [27], robotics and vehicle navigation and military applications. Early approaches that rely on decentralized organization can be found in Beni [9,15] and references therein. The related field of cooperative robotics is quite large; references and attempts to overview and classify the numerous publications can be found in Dudek et al. [23], Cao et al. [16], Liu and Passino [64]. Broader overviews on the topic of swarm intelligence are given in Bonabeau et al. [12] and Kennedy and Eberhardt [59]. In the references, a extensive list of works have been included. While these rule-driven paradigms are usually easy to construct, they are difficult to analyze mathematically. It is primarily for this reason that a mechanical approach is adopted here.

**Remark.** There is an extremely close area to this field, namely the study of "granular" or "particulate" media. Classical examples include the study of natural materials, such as sand and gravel, associated with coastal erosion, landslides and avalanches. A concise introduction is given by Duran [25]. Many man-made materials also fall within this class of problems. For general overviews of granular media, we refer the reader to Jaeger and Nagel [47,48], Nagel [67], Liu et al. [62], Liu and Nagel [63], Jaeger and Nagel [49], Jaeger et al. [50–52], Jaeger and Nagel [53], the extensive works of Hutter and collaborators: Tai et al. [80–82], Gray et al. [33], Wieland et al. [85], Berezin et al. [10], Gray and Hutter [34], Gray [35], Hutter [43], Hutter et al. [44], Hutter and Rajagopal [45], Koch et al. [60], Greve and Hutter [36] and Hutter et al. [46]; the works of Behringer and collaborators: Behringer [5], Behringer and Baxter [4], Behringer and Miller [6] and Behringer et al. [7]; the works of Jenkins and collaborators: Jenkins and Strack [54], Jenkins and La Ragione [55], Jenkins and Koenders [56], Jenkins et al. [57], the works of Torquato and collaborators: Torquato [83], Kansaal et al. [58] and Donev et al. [18–22] and the works of Zohdi and coworkers [86–97].

## 2. Basic modeling of "point-mass swarms

Throughout the analysis, the objects are assumed to be small enough to be considered (idealized) as point-masses and that the effects of their rotation with respect to their mass center is considered unimportant to their overall motion.

### 2.1. Notation

In this work, boldface symbols imply vectors or tensors. *A fixed Cartesian coordinate system will be used throughout this work*. The unit vectors for such a system are given by the mutually orthogonal triad of unit vectors $(\boldsymbol{e}_1, \boldsymbol{e}_2, \boldsymbol{e}_3)$. We denote the position of a point in space by the vector $\boldsymbol{r}$. In fixed Cartesian coordinates we have

$$\boldsymbol{r} = r_1\boldsymbol{e}_1 + r_2\boldsymbol{e}_2 + r_3\boldsymbol{e}_3, \tag{2.1}$$

and for the velocity we have

$$\boldsymbol{v} = \dot{\boldsymbol{r}} = \dot{r}_1\boldsymbol{e}_1 + \dot{r}_2\boldsymbol{e}_2 + \dot{r}_3\boldsymbol{e}_3, \tag{2.2}$$

and acceleration we have

$$\boldsymbol{a} = \ddot{\boldsymbol{r}} = \ddot{r}_1\boldsymbol{e}_1 + \ddot{r}_2\boldsymbol{e}_2 + \ddot{r}_3\boldsymbol{e}_3. \tag{2.3}$$

### 2.2. A basic construction of a swarm

In the analysis to follow, we treat the swarm members as point-masses, i.e. we ignore their dimensions.[2] For each swarm member ($N_p$ in total) the equations of motion are

$$m_i\ddot{\boldsymbol{r}}_i = \boldsymbol{\Psi}_i(\boldsymbol{r}_1, \boldsymbol{r}_2, \ldots, \boldsymbol{r}_{N_p}), \tag{2.4}$$

where $\boldsymbol{\Psi}$ represents the forces of interaction between swarm member $i$ and the target, obstacles, and other swarm members. We consider the following decomposition of interaction forces:

$$\boldsymbol{\Psi}_i = \boldsymbol{\Psi}_i^{mm} + \boldsymbol{\Psi}_i^{mt} + \boldsymbol{\Psi}_i^{mo}, \tag{2.5}$$

where between swarm members (member–member)

$$\boldsymbol{\Psi}_i^{mm} = \sum_{j\neq i}^{N_p} \left( \underbrace{\left( \underbrace{\alpha_1^{mm}\|\boldsymbol{r}_i - \boldsymbol{r}_j\|^{\beta_1^{mm}}}_{\text{attraction}} - \underbrace{\alpha_2^{mm}\|\boldsymbol{r}_i - \boldsymbol{r}_j\|^{-\beta_2^{mm}}}_{\text{repulsion}} \right)}_{\text{magnitude}} \underbrace{\frac{\boldsymbol{r}_j - \boldsymbol{r}_i}{\|\boldsymbol{r}_i - \boldsymbol{r}_j\|}}_{\boldsymbol{n}_{ij} \stackrel{\text{def}}{=} \text{unit vector}} \right), \tag{2.6}$$

where $\|\cdot\|$ represents the Euclidean norm in $R^3$, and the normal direction is determined by the difference in the position vectors of the particles' centers

$$\boldsymbol{n}_{ij} \stackrel{\text{def}}{=} \frac{\boldsymbol{r}_j - \boldsymbol{r}_i}{\|\boldsymbol{r}_i - \boldsymbol{r}_j\|}. \tag{2.7}$$

Between the swarm members and the target we have (member–target)

$$\boldsymbol{\Psi}_i^{mt} = (\alpha^{mt}\|\boldsymbol{r}_i - \boldsymbol{T}\|^{\beta^{mt}}) \frac{\boldsymbol{T} - \boldsymbol{r}_i}{\|\boldsymbol{r}_i - \boldsymbol{T}\|}, \tag{2.8}$$

and for the repulsion between swarm members and the obstacles (member–obstacle)

$$\boldsymbol{\Psi}^{mo} = -\sum_{j=1}^{q} \left( (\alpha^{mo}\|\boldsymbol{r}_i - \boldsymbol{O}_j\|^{-\beta^{mo}}) \frac{\boldsymbol{O}_j - \boldsymbol{r}_i}{\|\boldsymbol{r}_i - \boldsymbol{O}_j\|} \right), \tag{2.9}$$

where $q$ is the number of obstacles and where all of the (design) parameters, $\alpha$'s and $\beta$'s, are nonnegative.

**Remark 1.** One can describe the relative contributions of repulsion and attraction between members of the swarm by considering an individual pair in (static) equilibrium

$$\boldsymbol{\Psi}^{mm} = (\alpha_1^{mm}\|\boldsymbol{r}_i - \boldsymbol{r}_j\|^{\beta_1^{mm}} - \alpha_2^{mm}\|\boldsymbol{r}_i - \boldsymbol{r}_j\|^{-\beta_2^{mm}}) \frac{\boldsymbol{r}_j - \boldsymbol{r}_i}{\|\boldsymbol{r}_i - \boldsymbol{r}_j\|} = \boldsymbol{0}. \tag{2.10}$$

This characterizes a separation length scale describing the tendency to cluster or spread apart

$$\|\boldsymbol{r}_i - \boldsymbol{r}_j\| = \left(\frac{\alpha_2^{mm}}{\alpha_1^{mm}}\right)^{\frac{1}{\beta_1^{mm}+\beta_2^{mm}}} \stackrel{\text{def}}{=} d_e^{mm}. \tag{2.11}$$

*If the distance by which the swarm members can communicate is denoted $d^{com}$, and $d^{com} \leqslant d_e^{mm}$, then there will possibly be no interaction, for example at static equilibrium.*

**Remark 2.** The specific structure of the inter-particle forces chosen is only one of many possibilities to model the interaction. There are numerous other possibilities. The properties of this specific type of representation, such as the work expenditure, energy and power are discussed in the appendix. There are a variety of alternative forms available from the field of Molecular Dynamics (MD), which is concerned with, typically, the calculation of thermochemical and thermomechanical properties of gases, liquids and solids by using models of systems of atoms or molecules where each atom (or molecule) is represented by a material point and is treated as a point-mass whose motion is described by the Newton's second law with the forces computed from a prescribed potential energy function, $V(\boldsymbol{r}), m\ddot{\boldsymbol{r}} = -\nabla V(\boldsymbol{r})$ (see Haile [37], for example).

[2] The swarm member centers, which are initially non-intersecting, cannot intersect later due to the singular repulsion terms.

### 2.3. Environmental damping

A source of damping for the system is from the (surrounding) environment (for example, a fluid such as air). The simplest model is of the form (for swarm member $i$)

$$\boldsymbol{\Psi}_i^{env} = -c^{env}(\boldsymbol{v}_i - \boldsymbol{v}^{env}), \tag{2.12}$$

where $\boldsymbol{v}_i$ is the velocity of the $i$th member and $\boldsymbol{v}^{env}$ is the local velocity of the ambient medium. Im summary, we have the following forces acting on each member of the swarm:

$$\boldsymbol{\Psi} = \boldsymbol{\Psi}^{mm} + \boldsymbol{\Psi}^{mt} + \boldsymbol{\Psi}^{mo} + \boldsymbol{\Psi}^{env}. \tag{2.13}$$

**Remark.** The problem of fully coupled (two-way) particle-fluid interaction is beyond the scope of the present work. Generally, this requires the use of staggering-type schemes [95,97].

## 3. Temporal discretization

We now specifically address the second-order systems of interest.

### 3.1. Isolating a single particle

Each particle's equation of motion is given by

$$m\dot{\boldsymbol{v}} = \boldsymbol{\Psi}, \tag{3.1}$$

where $\boldsymbol{\Psi}$ is the force provided from interactions with other particles the external environment. Expanding the velocity in a Taylor series about $t + \phi\Delta t$ we obtain $(0 \leqslant \phi \leqslant 1)$

$$\boldsymbol{v}(t+\Delta t) = \boldsymbol{v}(t+\phi\Delta t) + \left.\frac{d\boldsymbol{v}}{dt}\right|_{t+\phi\Delta t}(1-\phi)\Delta t + \left.\frac{1}{2}\frac{d^2\boldsymbol{v}}{dt^2}\right|_{t+\phi\Delta t}(1-\phi)^2(\Delta t)^2 + \mathcal{O}(\Delta t)^3 \tag{3.2}$$

and

$$\boldsymbol{v}(t) = \boldsymbol{v}(t+\phi\Delta t) - \left.\frac{d\boldsymbol{v}}{dt}\right|_{t+\phi\Delta t}\phi\Delta t + \left.\frac{1}{2}\frac{d^2\boldsymbol{v}}{dt^2}\right|_{t+\phi\Delta t}\phi^2(\Delta t)^2 + \mathcal{O}(\Delta t)^3. \tag{3.3}$$

Subtracting the two expressions yields

$$\left.\frac{d\boldsymbol{v}}{dt}\right|_{t+\phi\Delta t} = \frac{\boldsymbol{v}(t+\Delta t) - \boldsymbol{v}(t)}{\Delta t} + \widehat{\mathcal{O}}(\Delta t), \tag{3.4}$$

where $\widehat{\mathcal{O}}(\Delta t) = \mathcal{O}(\Delta t)^2$ when $\phi = \frac{1}{2}$. Inserting this into the equation of motion yields

$$\boldsymbol{v}(t+\Delta t) = \boldsymbol{v}(t) + \frac{\Delta t}{m}\boldsymbol{\Psi}(t+\phi\Delta t) + \widehat{\mathcal{O}}(\Delta t)^2. \tag{3.5}$$

Note that adding a weighted sum of Eqs. (3.2) and (3.3) yields

$$\boldsymbol{v}(t+\phi\Delta t) = \phi\boldsymbol{v}(t+\Delta t) + (1-\phi)\boldsymbol{v}(t) + \mathcal{O}(\Delta t)^2, \tag{3.6}$$

which will be useful shortly. Now expanding the position of the center of mass in a Taylor series about $t + \phi\Delta t$ we obtain

$$\boldsymbol{r}(t+\Delta t) = \boldsymbol{r}(t+\phi\Delta t) + \left.\frac{d\boldsymbol{r}}{dt}\right|_{t+\phi\Delta t}(1-\phi)\Delta t + \left.\frac{1}{2}\frac{d^2\boldsymbol{r}}{dt^2}\right|_{t+\phi\Delta t}(1-\phi)^2(\Delta t)^2 + \mathcal{O}(\Delta t)^3 \tag{3.7}$$

and

$$\boldsymbol{r}(t) = \boldsymbol{r}(t+\phi\Delta t) - \left.\frac{d\boldsymbol{r}}{dt}\right|_{t+\phi\Delta t}\phi\Delta t + \left.\frac{1}{2}\frac{d^2\boldsymbol{r}}{dt^2}\right|_{t+\phi\Delta t}\phi^2(\Delta t)^2 + \mathcal{O}(\Delta t)^3. \tag{3.8}$$

Subtracting the two expressions yields

$$\frac{\boldsymbol{r}(t+\Delta t) - \boldsymbol{r}(t)}{\Delta t} = \boldsymbol{v}(t+\phi\Delta t) + \widehat{\mathcal{O}}(\Delta t). \tag{3.9}$$

Inserting Eq. (3.6) yields

$$\boldsymbol{r}(t+\Delta t) = \boldsymbol{r}(t) + (\phi\boldsymbol{v}(t+\Delta t) + (1-\phi)\boldsymbol{v}(t))\Delta t + \widehat{\mathcal{O}}(\Delta t)^2 \tag{3.10}$$

and thus using Eq. (3.5) yields

$$\boldsymbol{r}(t+\Delta t) = \boldsymbol{r}(t) + \boldsymbol{v}(t)\Delta t + \frac{\phi(\Delta t)^2}{m}\boldsymbol{\Psi}(t+\phi\Delta t) + \widehat{\mathcal{O}}(\Delta t)^2. \tag{3.11}$$

The term $\boldsymbol{\Psi}(t+\phi\Delta t)$ can be approximated by

$$\boldsymbol{\Psi}(t+\phi\Delta t) \approx \phi\boldsymbol{\Psi}(\boldsymbol{r}(t+\Delta t)) + (1-\phi)\boldsymbol{\Psi}(\boldsymbol{r}(t)), \tag{3.12}$$

yielding

$$\boldsymbol{r}(t+\Delta t) = \boldsymbol{r}(t) + \boldsymbol{v}(t)\Delta t + \frac{\phi(\Delta t)^2}{m}(\phi\boldsymbol{\Psi}(\boldsymbol{r}(t+\Delta t)) + (1-\phi)\boldsymbol{\Psi}(\boldsymbol{r}(t))) + \widehat{\mathcal{O}}(\Delta t)^2. \tag{3.13}$$

We note that

- When $\phi = 1$, then this is the (implicit) Backward Euler scheme, which is very stable (very dissipative) and $\mathcal{O}(\Delta t)^2$ locally in time,
- When $\phi = 0$, then this is the (explicit) Forward Euler scheme, which is conditionally stable and $\mathcal{O}(\Delta t)^2$ locally in time,
- When $\phi = 0.5$, then this is the (implicit) "Midpoint" scheme, which is stable and $\widehat{\mathcal{O}}(\Delta t)^2 = \mathcal{O}(\Delta t)^3$ locally in time.

### 3.2. Iterative solution methods for coupled systems

We now develop an adaptive iterative scheme for the coupled system by following an approach found in Zohdi [86–88]. Implicit time stepping methods, with time step size adaptivity, built on approaches found in Zohdi [87], will be used throughout the upcoming analysis. For illustration purposes, after time discretization of the acceleration term in the equations of motion $m\ddot{\boldsymbol{r}} = \boldsymbol{\Psi}$ using a $\phi$-method

$$\boldsymbol{r}^{L+1} = \boldsymbol{r}^L + \boldsymbol{v}^L\Delta t + \frac{\phi(\Delta t)^2}{m}(\phi\boldsymbol{\Psi}(\boldsymbol{r}^{L+1}) + (1-\phi)\boldsymbol{\Psi}(\boldsymbol{r}^L)), \tag{3.14}$$

one arrives at the following abstract form, for the entire system of particles,

$$\mathscr{A}(\boldsymbol{r}^{L+1}) = \mathscr{F}. \tag{3.15}$$

It is convenient to write

$$\mathscr{A}(\boldsymbol{r}^{L+1}) - \mathscr{F} = \mathscr{G}(\boldsymbol{r}^{L+1}) - \boldsymbol{r}^{L+1} + \mathscr{R} = \boldsymbol{0}, \tag{3.16}$$

where $\mathscr{R}$ is a remainder term that does not depend on the solution, i.e. $\mathscr{R} \neq \mathscr{R}(\boldsymbol{r}^{L+1})$. A straightforward iterative scheme can be written as

$$\boldsymbol{r}^{L+1,K} = \mathscr{G}(\boldsymbol{r}^{L+1,K-1}) + \mathscr{R}, \tag{3.17}$$

where $K = 1, 2, 3, \ldots$ is the index of iteration within time step $L+1$. The convergence of such a scheme is dependent on the behavior of $\mathscr{G}$. Namely, a sufficient condition for convergence is that $\mathscr{G}$ is a contraction mapping for all $\boldsymbol{r}^{L+1,K}$, $K = 1, 2, 3, \ldots$ In order to investigate this further, we define the iteration error as $\varepsilon^{L+1,K} \stackrel{\text{def}}{=} \boldsymbol{r}^{L+1,K} - \boldsymbol{r}^{L+1}$. A necessary restriction for convergence is iterative self consistency,

i.e. the "exact" (discretized) solution must be represented by the scheme

$$\mathscr{G}(\boldsymbol{r}^{L+1}) + \mathscr{R} = \boldsymbol{r}^{L+1}. \tag{3.18}$$

Enforcing this restriction, a sufficient condition for convergence is the existence of a contraction mapping

$$\begin{aligned} \varepsilon^{L+1,K} &= \|\boldsymbol{r}^{L+1,K} - \boldsymbol{r}^{L+1}\| = \|\mathscr{G}(\boldsymbol{r}^{L+1,K-1}) - \mathscr{G}(\boldsymbol{r}^{L+1})\|, &(3.19)\\ &\leqslant \eta^{L+1,K}\|\boldsymbol{r}^{L+1,K-1} - \boldsymbol{r}^{L+1}\|, &(3.20)\end{aligned}$$

where if $0 \leqslant \eta^{L+1,K} < 1$ for each iteration $K$, then $\varepsilon^{L+1,K} \to \mathbf{0}$ for any arbitrary starting value $\boldsymbol{r}^{L+1,K=0}$, as $K \to \infty$. This type of contraction condition is sufficient, but not necessary, for convergence. Inserting this into $m\ddot{\boldsymbol{r}} = \boldsymbol{\Psi}(\boldsymbol{r})$ leads to

$$\boldsymbol{r}^{L+1,K} = \underbrace{\boldsymbol{r}^{L} + \boldsymbol{v}^{L}\Delta t + \frac{\phi(\Delta t)^2}{m}((1-\phi)\boldsymbol{\Psi}(\boldsymbol{r}^{L}))}_{\mathscr{R}} + \underbrace{\frac{\phi(\Delta t)^2}{m}(\phi\boldsymbol{\Psi}(\boldsymbol{r}^{L+1,K-1}))}_{\mathscr{G}(\boldsymbol{r}^{L+1,K-1})}, \tag{3.21}$$

whose convergence is restricted by $\eta \propto \frac{(\phi\Delta t)^2}{m}$. Therefore, we see that the contraction constant of $\mathscr{G}$ is (1) directly dependent on the strength of the interaction forces, (2) inversely proportional to $m$ and (3) directly proportional to $\phi\Delta t$. Therefore, if convergence is slow within a time step, the time step size, which is adjustable, can be reduced by an appropriate amount to increase the rate of convergence. Thus, decreasing the time step size improves the convergence, however, we want to simultaneously maximize the time step sizes to decrease overall computing time, while still meeting an error tolerance on the numerical solution's accuracy. In order to achieve this goal, we follow an approach found in Zohdi [86,87] originally developed for continuum thermochemical multifield problems in which (1) one approximates

$$\eta^{L+1,K} \approx S(\Delta t)^p \tag{3.22}$$

($S$ is a constant) and (2) one assumes that the error within an iteration to behave according to

$$(S(\Delta t)^p)^K \varepsilon^{L+1,0} = \varepsilon^{L+1,K}, \quad K = 1,2,\ldots \tag{3.23}$$

where $\varepsilon^{L+1,0}$ is the initial norm of the iterative error and $S$ is intrinsic to the system.[3] Our goal is to meet an error tolerance in exactly a preset number of iterations. To this end, one writes

$$(S(\Delta t_{\text{tol}})^p)^{K_d} \varepsilon^{L+1,0} = TOL, \tag{3.24}$$

where $TOL$ is a tolerance and where $K_d$ is the number of desired iterations.[4] If the error tolerance is not met in the desired number of iterations, the contraction constant $\eta^{L+1,K}$ is too large. Accordingly, one can solve for a new smaller step size, under the assumption that $S$ is constant,

$$\Delta t_{\text{tol}} = \Delta t \left( \frac{\left(\frac{TOL}{\varepsilon^{L+1,0}}\right)^{\frac{1}{pK_d}}}{\left(\frac{\varepsilon^{L+1,K}}{\varepsilon^{L+1,0}}\right)^{\frac{1}{pK}}} \right). \tag{3.25}$$

The assumption that $S$ is constant is not critical, since the time steps are to be recursively refined and unrefined throughout the simulation. Clearly, the expression in Eq. (3.25) can also be used for time step enlargement, if convergence is met in less than $K_d$ iterations.[5] An implementation of the procedure is as follows:

(1) GLOBAL FIXED − POINT ITERATION : (SET i = 1 AND K = 0) :
(2) IF i > $N_p$ THEN GO TO (4)
(3) IF i ≤ $N_p$ THEN :
  ($a$) COMPUTE POSITION :$\boldsymbol{r}_i^{L+1,K}$
  ($b$) GO TO (2) FOR NEXT SWARM MEMBER (i = i + 1)
(4) ERROR MEASURE :
  ($a$)$\varepsilon_K \overset{\text{def}}{=} \frac{\sum_{i=1}^{N_p} ||\boldsymbol{r}_i^{L+1,K} - \boldsymbol{r}_i^{L+1,K-1}||}{\sum_{i=1}^{N_p} ||\boldsymbol{r}_i^{L+1,K} - \boldsymbol{r}_i^{L}||}$ (normalized)
  ($b$)$Z_K \overset{\text{def}}{=} \frac{\varepsilon_K}{TOL_r}$
  ($c$)$\Phi_K \overset{\text{def}}{=} \left( \frac{(\frac{TOL}{\varepsilon_0})^{\frac{1}{pK_d}}}{(\frac{\varepsilon_K}{\varepsilon_0})^{\frac{1}{pK}}} \right)$
(5) IF TOLERANCE MET ($Z_K \leq 1$) AND $K < K_d$ THEN :
  ($a$) INCREMENT TIME : $t = t + \Delta t$
  ($b$) CONSTRUCT NEW TIME STEP : $\Delta t = \Phi_K \Delta t$,
  ($c$) SELECT MINIMUM : $\Delta t = MIN(\Delta t^{lim}, \Delta t)$ AND GO TO (1)
(6) IF TOLERANCE NOT MET ($Z_K > 1$) AND $K = K_d$ THEN :
  ($a$) CONSTRUCT NEW TIME STEP :$\Delta t = \Phi_K \Delta t$
  ($b$) RESTART AT TIME = t AND GO TO (1)

(3.26)

Generally speaking, the iterative error, which is a function of the time step size, is temporally variable and can become stronger, weaker, or possibly oscillatory, is extremely difficult to ascertain a priori as a function of the time step size. Therefore, to circumvent this problem, the adaptive strategy presented in this section was developed to provide accurate solutions by iteratively adjusting the time steps. Specifically, a sufficient condition for the convergence of the presented fixed-point scheme was that the spectral radius or contraction constant of the coupled operator, which depends on the time step size, must be less than unity. This observation was used to adaptively maximize the time step sizes, while simultaneously controlling the coupled operator's spectral radius, in order to deliver solutions below an error tolerance within a prespecified number of desired iterations. This recursive staggering error control can allow for substantial reduction of computational effort by the adaptive use of large time steps. Furthermore, such a recursive process has a reduced sensitivity, relative to an explicit staggering approach, to the order in which the individual equations are solved, since it is self-correcting. For extensive parameter studies on this approach see Zohdi [97].

**Remark.** With regard to the solution process, a recursive iterative scheme of the Jacobi-type, where the updates are made only after one complete system iteration, was illustrated in the derivations only for algebraic simplicity. The Jacobi method is easier to address theoretically, while the Gauss–Seidel type method, which involves immediately using the most current values, when they become available, is usually used at the implementation level. As is well known, under relatively general conditions, if the Jacobi method converges, the Gauss–Seidel method converges at a faster rate, while if the Jacobi method diverges, the Gauss–Seidel method diverges at a faster rate (for example, see Ames [1] or Axelsson [2]). It is important to realize that the Jacobi method is perfectly parallelizable. In other words, the calculation for each particle are uncoupled, with the updates only coming afterward. Gauss–Seidel, since it requires the most current updates, couples the particle calculations immediately. However, these methods can be combined to create hybrid approaches, whereby the entire particulate flow is partitioned into groups and within each group a Gauss–Seidel method is applied. In other words, for a group, the positions of any particles from outside are initially frozen, as far as calculations involving members of the group are concerned. After each isolated group's solution (particle positions) has converged, computed in parallel, then all positions are updated, i.e. the most current positions become available to all members of the swarm, and the isolated group calculations are repeated. Classical solution methods require $\mathcal{O}(N^3)$ operations, whereas iterative schemes,

[3] For the class of problems under consideration, due to the quadratic dependency on $\Delta t$, $p \approx 2$.

[4] Typically, $K_d$ is chosen to be between five to ten iterations.

[5] Time step size adaptivity is important, since the system's dynamics can dramatically change over the course of time, possibly requiring quite different time step sizes to control the iterative error. However, to maintain the accuracy of the time stepping scheme, one must respect an upper bound dictated by the discretization error, i.e., $\Delta t \leqslant \Delta t^{lim}$.

such as the one presented, typically require order $N^q$, where $1 \leqslant q \leqslant 2$. For details see Axelsson [2]. Also, such solvers are highly advantageous since solutions to previous time steps can be used as the first guess to accelerate the solution procedure.

## 4. Numerical examples

### 4.1. A model problem: chasing a moving target

As a representative of a class of model problems, we now consider a normalized "performance" function (normalized by the total simulation time and the initial separation distance) representing (1) the time it takes for the swarm members to get to the target and (2) the distance of the swarm members away from the target:

$$\Pi = \frac{\left(\int_0^{\mathscr{T}} \sum_{i=1}^{N_p} \|\boldsymbol{r}_i - \boldsymbol{T}\| \, dt\right)}{\mathscr{T} \sum_{i=1}^{N_p} \|\boldsymbol{r}_i(t=0) - \boldsymbol{T}\|}, \tag{4.1}$$

where total simulation time is $\mathscr{T} = 30$ and $\boldsymbol{T}$ is the position of the target (Fig. 1). The components of the initial position vectors of the non-intersecting swarm members, each assigned a mass of 10 kg. were given random values of $-1 \leqslant r_{ix},\ r_{iy},\ r_{iz} \leqslant 1$. The location of the *moving* target was given by the following function:

$$\begin{aligned} T_x &= x_o + a_1 cos(a_2 t) + a_3 t, \\ T_y &= y_o + b_1 sin(b_2 t) + b_3 t, \\ T_z &= z_o + c_1 cos(c_2 t) + c_3 t. \end{aligned} \tag{4.2}$$

The location of the center of the (rectangular) obstacle array was (1.5,0,0). A 100-obstacle "fence" was set up in a $10 \times 10$ array with a spacing of 0.2 between obstacle centers. For illustration purposes, 200 swarm members were used. The parameters selected were: $\alpha_1^{mm} = 1,\ \alpha_2^{mm} = 1,\ \alpha^{mt} = 200,\ \alpha^{mo} = 100,\ \beta_1^{mm} = 2,\ \beta_2^{mm} = 2,\ \beta^{mt} = 2$ and $\beta^{mo} = 2$. The environmental damping was set to $c^{env} = 1$. The total time was set to $\mathscr{T} = 30$. Simulations, shown in Fig. 2, were run with the performance being $\Pi = 0.2712$ (Time steps: 3439, Fixed-Point iterations: 24633). Although there is environmental damping, the envelope of motion is quite large initially (see Table 1).

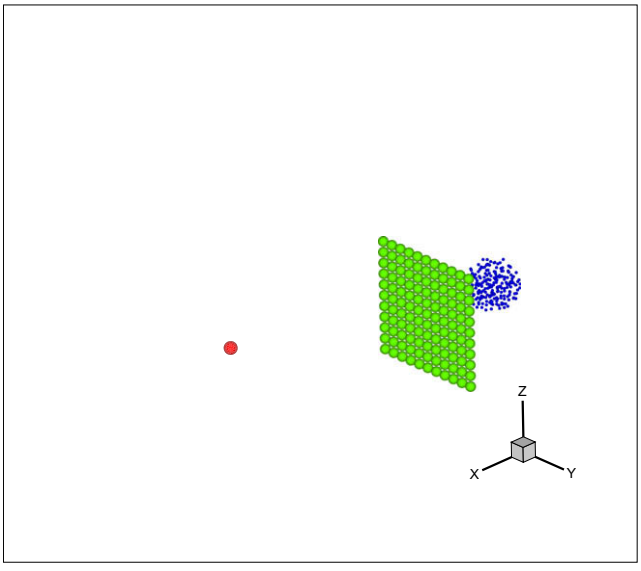


**Fig. 1.** A typical setup for a "swarm". The target is shown in red, the obstacles in green and the swarm members are shown in blue. (For interpretation of the references in colour in this figure legend, the reader is referred to the web version of this article.)

**Remark 1.** Typically, for systems with a finite number of particles, there will be slight variations in the performance for different random starting configurations. In order to stabilize the objective function's value with respect to the randomness of the flow starting configuration, for a given parameter selection ($\boldsymbol{\Lambda}$, characterized by the $\alpha$'s and $\beta$'s), a regularization procedure is applied, whereby the performances of a series of different random starting configurations are averaged until the (ensemble) average converges, i.e. until the following condition is met:

$$\left| \frac{1}{E+1} \sum_{i=1}^{E+1} \Pi^{(i)}(\boldsymbol{\Lambda}^I) - \frac{1}{E} \sum_{i=1}^{E} \Pi^{(i)}(\boldsymbol{\Lambda}^I) \right| \leqslant TOL \left| \frac{1}{E+1} \sum_{i=1}^{E+1} \Pi^{(i)}(\boldsymbol{\Lambda}^I) \right|, \tag{4.3}$$

where index $i$ indicates a different starting random configuration ($i = 1, 2, \ldots, E$) that has been generated and $E$ indicates the total number of configurations tested. For swarms of the sizes tested, typically, on 2 or 3 samples realizations were needed to average over.

**Remark 2.** In Zohdi [87], different sized swarms were tested, and the resulting optimal strategies (attraction and repulsion coefficients) were tabulated. From those results it became clear that in some cases, if the swarm is small enough, bunching up and moving through the obstacle course is the optimal strategy. Generally, the best strategy depends strongly on the obstacle course size and shape and swarm size. A strategy for estimating the parameters, based on genetic algorithms, is given in the appendix.

**Remark 3.** In many applications the interaction can dramatically change when the particles are very close to one another, leading to increased attraction, resulting in clustering and agglomeration. A particularly easy way to model this is via an attractive augmentation of the form

$$\boldsymbol{\Psi}_i = \boldsymbol{\Psi}_i + \underbrace{\alpha_a \|\boldsymbol{r}_i - \boldsymbol{r}_j\|^{\beta_a} \boldsymbol{n}_{ij}}_{\boldsymbol{\Psi}^a \stackrel{\text{def}}{=} \text{BINDING FORCE}}, \tag{4.4}$$

which is activated if

$$\|\boldsymbol{r}_i - \boldsymbol{r}_j\| \leqslant (b_i + b_j)\delta_a, \tag{4.5}$$

where $b_i$ and $b_j$ are the radii of the particles,[6] and where $1 \leqslant \delta_a$ is the critical distance needed for the augmentation to become active. Denoting the nominal (unagglomerated) equilibrium distance by $d_e$ and the equilibrium distance when agglomeration is active, by $d_a$, we have, with $\beta_a = \beta_1$

$$\|\boldsymbol{r}_i - \boldsymbol{r}_j\| = \left(\frac{\alpha_2}{\alpha_1 + \alpha_a}\right)^{\frac{1}{\beta_1 + \beta_2}} = d_a \leqslant d_e = \left(\frac{\alpha_2}{\alpha_1}\right)^{\frac{1}{\beta_1 + \beta_2}}. \tag{4.6}$$

**Remark 4.** If we wish to enforce that, if a swarm member gets too close to an obstacle, then it becomes immobilized, a side condition can be introduced of the form, $\forall t, \forall r_{oj}$ and $\tau < \mathscr{T}$, if

$$\|\boldsymbol{r}_i(t=\tau) - \boldsymbol{O}_j\| \leqslant R \tag{4.7}$$

then $\boldsymbol{r}_i = \boldsymbol{r}_i(t=\tau),\ \forall t \geqslant \tau$, where the unilateral condition represents the effect of being near a "destructive" obstacle. The swarm member is stopped in the position where it enters the "radius of destruction" ($R$). Therefore, the swarm performance ($\Pi$) is severely penalized if it loses members to the obstacles.

[6] They will be taken to be the same, later in the simulations.

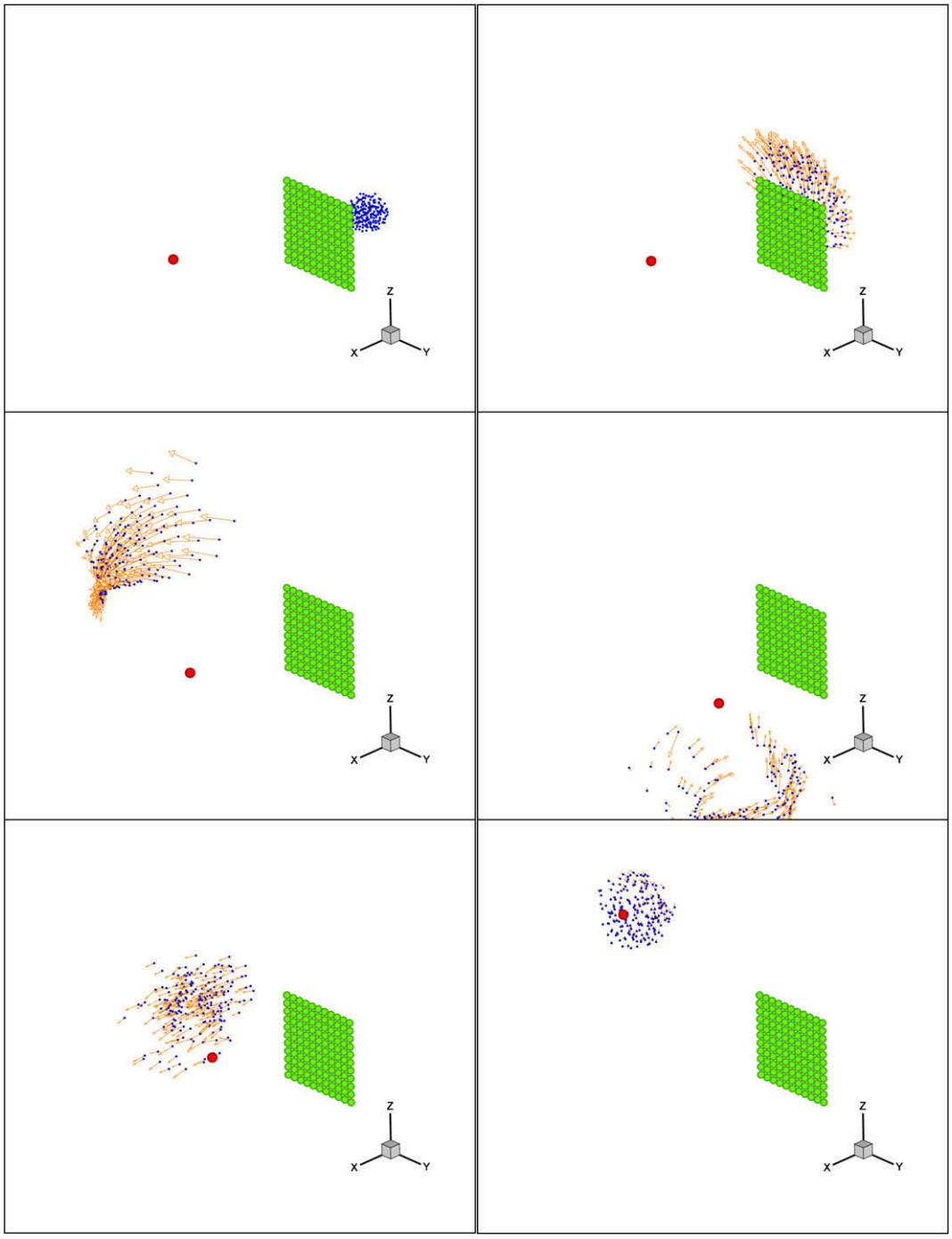


**Fig. 2.** Top to bottom and left to right, the swarm moves over the obstacle fence.

**Table 1**
Table of parameters.

| $(x_o, y_o, z_o)$ | $a_1$ | $a_2$ | $a_3$ | $b_1$ | $b_2$ | $b_3$ | $c_1$ | $c_2$ | $c_3$ |
|---|---|---|---|---|---|---|---|---|---|
| (4,0,0) | 1 | 1 | 0.5 | 1 | 1 | 0.5 | 1 | 1 | 0.5 |

**Remark 5.** It is important to note that if the interaction is only between the nearest neighbors, and if there is no inertial reference point for the swarm members to refer to, instabilities (collisions) may occur [40,41,76,78,79]. In the present analysis, such inertial reference points were provided by the swarm's knowledge of the stationary obstacles and target.

### *4.2. Another model problem: multi-site search*

As another a model problem, consider 400 swarm members and 200 randomly dispersed "target sites" which the swarm is tasked to visit (Fig. 3). The algorithm is as follows: (1) Each swarm member is attracted to the nearest target location and (2) If a site has been visited, then it is inactive (the swarm is not attracted to it). As the frames indicate, the swarm has a natural tendency to divide and conquer the domain.

**Remark.** There are over 100,000,000,000 websites as of 2007. There are, on average, approximately 250 words per page (like a book). Clearly, searches for a piece of information would take a

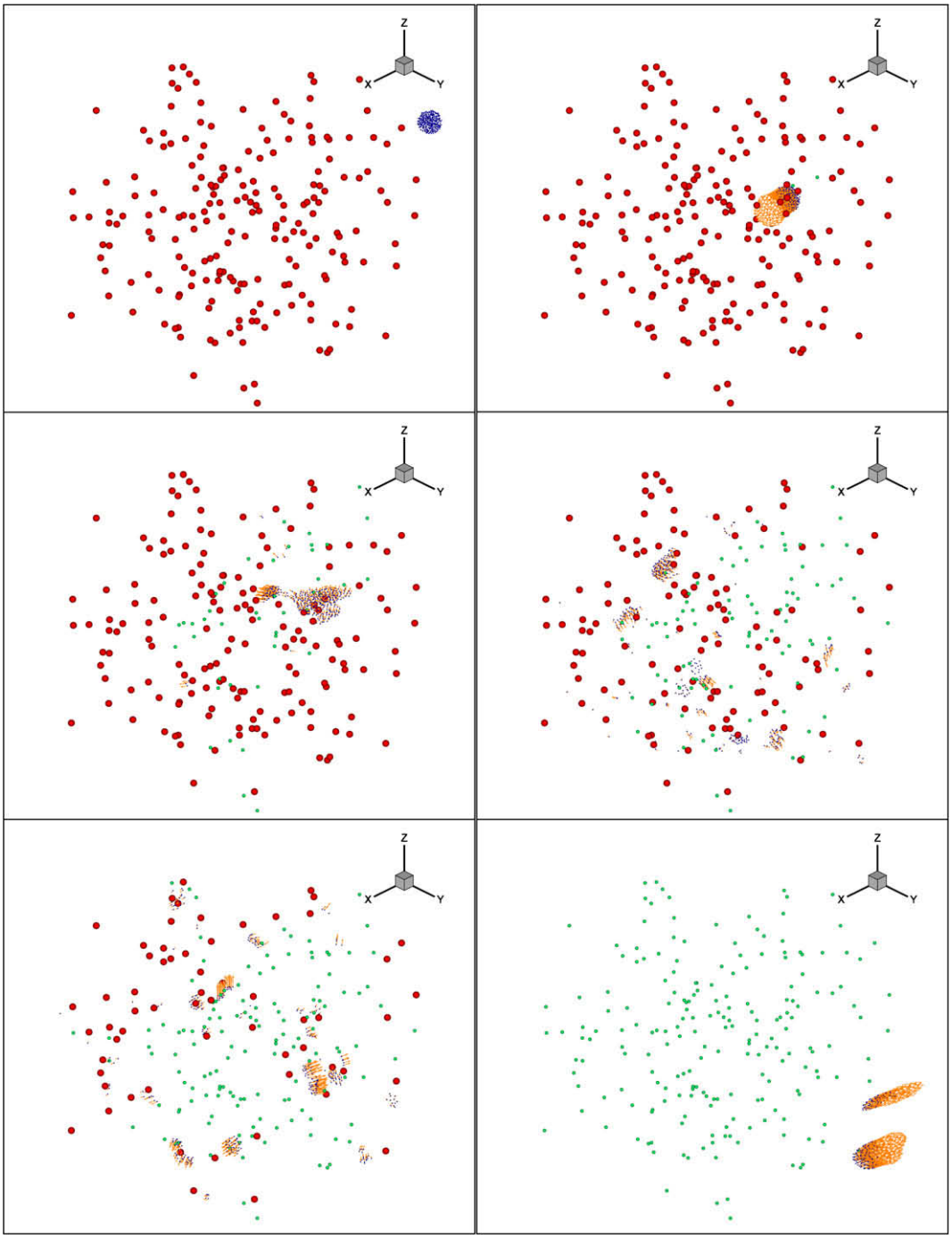


**Fig. 3.** Top to bottom and left to right, the swarm moves through the search space. Red = site unvisited and green = site visited. (For interpretation of the references in colour in this figure legend, the reader is referred to the web version of this article.)

very long time if done directly. Since a computer cannot recognize words and sentences, only bytes, this requires specialized natural language processing algorithms, which incorporate programs for parsing. In this regard, there are processes such as "web-crawling" or "spidering". These approaches systematically browse the net in an automated fashion. These programs are primarily used to create a copy of all visited pages for later processing by a search engine. It is hoped that swarm-type search, if adapted properly, and combined with a proper web-crawling routines, could provide a new, hopefully faster, search paradigm. Primarily, here we mean by search (both virtual and physical): (1) *Data mining* for informational queries (via the internet), (2) *Multi-pronged cloud-type search*: circumvents the slower tree-type data structure search and (3) *Area-coverage/man-overboard search:* determination of optimal paths for maximum area-coverage, for example, for a lost object.

## 5. Discussion and concluding remarks

In many applications, the computed positions, velocities and accelerations of the members of a swarm, for example people or vehicles, must be translated into realizable movement. Furthermore, the communication latency and information exchange poses

a significant technological hurdle. In practice, further sophistication, i.e. constraints on movement and communication, must be embedded into the computational model for the application at hand. However, the fundamental computational philosophy and modeling strategy should remain relatively unchanged.

For certain types of swarms the "visual field" of the individual members may play a significant role in the overall behavior. In some cases, this is a non-issue, for example if the vehicles are robots or UAVs, since the communication is most likely electronic. However, for certain animals, they see only ahead of them. A relatively simple way to incorporate this into a simulation is to check the inner product of each swarm member's velocity with a neighbor's relative position vector, $(\boldsymbol{r}_j - \boldsymbol{r}_i) \cdot \boldsymbol{v}_i$. Under the assumption that the swarm members "look where they are going", if the inner product is negative, this indicates that the neighbor is behind the swarm member's visual field, and hence there is no interaction between this specific pair of swarm members. Also, it is important to note that some while groups interact with their nearest neighbors, while some with a specific number of swarm members, *regardless* of whether they are far away [26]. For example, specifically for Starlings (Sturnus vulgaris), Ballerini et al. [3] conclude, based on a number of careful observations, that interactions are governed by topological distance and not metric distance, i.e. a bird communicates with a certain number of birds surrounding it, *regardless of the distance away*. The authors believe that this may be attributed to a perceptual limit in of the number of objects that they can track. Specifically, Ballerini et al. [3] have determined that the interaction, for a typical bird in a swarm, decays rapidly after approximately the sixth or seventh nearest neighbor. For Starlings, their empirical evidence appears to support this hypothesis. This issue is currently under investigation by the author.

Finally, an important aspect of any model is the identification of parameters which force the system behavior to approximate, as close as possible, a desired target response. For example, in the ideal case, one would like to determine the type of interaction that produces certain overall system characteristics, via numerical simulations, in order to guide or minimize time-consuming laboratory tests. As a representative of a class of model problems, consider "inverse" problems whereby the parameters in the interaction representation are sought, the $\alpha$'s and $\beta$'s, which deliver a target system behavior by minimizing a normalized cost function

$$\Pi = \frac{\int_0^{\mathscr{T}} |A - A^*|\, dt}{\int_0^{\mathscr{T}} |A^*|\, dt}, \tag{5.1}$$

where the total simulation time is $\mathscr{T}$, where $A$ is a computationally generated quantity of interest and where $A^*$ is the target response. Typically, for the class of problems considered in this work, formulations $(\Pi)$ such as in Eq. (5.1) depend, in a nonconvex and nondifferentiable manner, on the $\alpha$'s and $\beta$'s. This is primarily due to the nonlinear character of the interaction, the physics of sudden inter-particle impact and the transient dynamics. Clearly, we must have restrictions (for physical reasons) on the parameters in the interaction

$$\alpha_i^- \leqslant \alpha_i \leqslant \alpha_i^+ \tag{5.2}$$

and

$$\beta_i^- \leqslant \beta_i \leqslant \beta_i^+, \tag{5.3}$$

where $\alpha_i^-$, $\alpha_i^+$, $\beta_i^-$ and $\beta_i^+$, are the lower and upper limits on the coefficients in the interaction forces.[7] With respect to the minimization of Eq. (5.1), classical gradient-based deterministic optimization techniques are not robust, due to difficulties with objective function nonconvexity and nondifferentiability. Classical gradient-based algorithms are likely to converge only toward a local minimum of the objective function unless a sufficiently close initial guess to the global minimum is not provided. Also, usually it is extremely difficult to construct an initial guess that lies within the (global) convergence radius of a gradient-based method. These difficulties can be circumvented by the use of a certain class of simple, yet robust, nonderivative search methods, usually termed "genetic" algorithms (GA), before applying gradient-based schemes. Genetic algorithms are search methods based on the principles of natural selection, employing concepts of species evolution, such as reproduction, mutation and crossover. Implementation typically involves a randomly generated population of fixed-length elemental strings, "genetic" information", each of which represents a specific choice of system parameters. The population of individuals undergo "mating sequences" and other biologically inspired events in order to find promising regions of the search space. There are a variety of such methods, which employ concepts of species evolution, such as reproduction, mutation and crossover. Such methods can be traced back, at least, to the work of John Holland [42]. For reviews of such methods, see, for example, Goldberg [31], Davis [17], Onwubiko [68], Kennedy and Eberhart [59] Lagaros et al. [61], Papadrakakis et al. [69–72] and Goldberg and Deb [32]. The appendix provides further information on the use of genetic algorithms.

## Appendix A. Fundamentals of potentials

When the dimensions of a body are insignificant to the description of its motion or the action of forces on it, the body may be idealized as a particle, i.e. a piece of material occupying a point in space and perhaps moving as times passes. In the next few sections, we briefly review some essential concepts that will be needed later in the analysis of particles.

### A.1. Work, energy and power

A closely related concept is that of work and energy. The differential amount of work done by a force acting through a differential displacement is

$$dW = \boldsymbol{\Psi} \cdot d\boldsymbol{r}. \tag{A.1}$$

Therefore, the total amount of work performed by a force over a displacement history is

$$\begin{aligned} W_{1\to 2} &= \int_{\boldsymbol{r}(t_1)}^{\boldsymbol{r}(t_2)} \boldsymbol{\Psi} \cdot d\boldsymbol{r} = \int_{\boldsymbol{r}(t_1)}^{\boldsymbol{r}(t_2)} m\boldsymbol{a} \cdot d\boldsymbol{r} = \int_{\boldsymbol{r}(t_1)}^{\boldsymbol{r}(t_2)} m\boldsymbol{v} \cdot d\boldsymbol{v} \\ &= \frac{1}{2} m(\boldsymbol{v}_2 \cdot \boldsymbol{v}_2 - \boldsymbol{v}_1 \cdot \boldsymbol{v}_1) \stackrel{\text{def}}{=} T_2 - T_1, \end{aligned} \tag{A.2}$$

where $T \stackrel{\text{def}}{=} \frac{1}{2} m\boldsymbol{v} \cdot \boldsymbol{v}$ is known as the kinetic energy.[8] Therefore, we may write

$$T_1 + W_{1\to 2} = T_2. \tag{A.3}$$

If the forces can be written in the following form:

$$dV = -\boldsymbol{\Psi} \cdot d\boldsymbol{r}, \tag{A.4}$$

then

$$W_{1\to 2} = -\int_{\boldsymbol{r}(t_1)}^{\boldsymbol{r}(t_2)} dV = V(\boldsymbol{r}(t_1)) - V(\boldsymbol{r}(t_2)), \tag{A.5}$$

where

$$\boldsymbol{\Psi} = -\nabla V. \tag{A.6}$$

[7] Additionally, we could also vary the other parameters in the system, such as the drag, etc. However, we shall fix these parameters during the upcoming examples.

[8] The chain rule was used to write $\boldsymbol{a} \cdot d\boldsymbol{r} = \boldsymbol{v} \cdot d\boldsymbol{v}$.

Such a force is said to be conservative. Furthermore, it is easy to show that a conservative force must satisfy

$$\nabla \times \boldsymbol{\Psi} = \mathbf{0}. \tag{A.7}$$

The work done by a conservative force on any closed path is zero, since

$$-\int_{\boldsymbol{r}(t_1)}^{\boldsymbol{r}(t_2)} dV = V(\boldsymbol{r}(t_1)) - V(\boldsymbol{r}(t_2)) = \int_{\boldsymbol{r}(t_2)}^{\boldsymbol{r}(t_1)} dV$$
$$\Rightarrow \int_{\boldsymbol{r}(t_1)}^{\boldsymbol{r}(t_2)} dV + \int_{\boldsymbol{r}(t_2)}^{\boldsymbol{r}(t_1)} dV = 0. \tag{A.8}$$

As a consequence, for a conservative system,

$$T_1 + V_1 = T_2 + V_2. \tag{A.9}$$

Also, power can be defined as the time rate of change of work

$$\frac{dW}{dt} = \frac{\boldsymbol{\Psi} \cdot d\boldsymbol{r}}{dt} = \boldsymbol{\Psi} \cdot \boldsymbol{v}. \tag{A.10}$$

### A.2. Properties of a potential

As we have indicated, a force field $\boldsymbol{\Psi}$ is said to be conservative if and only if there exists a continuously differentiable scalar field $V$ such that, $\boldsymbol{\Psi} = -\nabla V$. Therefore, a necessary and sufficient condition for a particle to be in equilibrium is that

$$\boldsymbol{\Psi} = -\nabla V = \mathbf{0}. \tag{A.11}$$

In other words

$$\frac{\partial V}{\partial x_1} = 0, \quad \frac{\partial V}{\partial x_2} = 0 \quad \text{and} \quad \frac{\partial V}{\partial x_3} = 0. \tag{A.12}$$

Forces acting on a particle that are (1) always directed toward or away another point and (2) whose magnitude depends only on the distance between the particle and the point of attraction/repulsion are called *central forces*. They have the form

$$\boldsymbol{\Psi} = -\mathscr{C}(\|\boldsymbol{r} - \boldsymbol{r}_o\|)\frac{\boldsymbol{r} - \boldsymbol{r}_o}{\|\boldsymbol{r} - \boldsymbol{r}_o\|} = \mathscr{C}(\|\boldsymbol{r} - \boldsymbol{r}_o\|)\boldsymbol{n}, \tag{A.13}$$

where $\boldsymbol{r}$ is the position of the particle, $\boldsymbol{r}_o$ is the position of a point to which the particle is attracted toward and repulsed from and

$$\boldsymbol{n} = \frac{\boldsymbol{r}_o - \boldsymbol{r}}{\|\boldsymbol{r} - \boldsymbol{r}_o\|}. \tag{A.14}$$

The central force is one of attraction if

$$\mathscr{C}(\|\boldsymbol{r} - \boldsymbol{r}_o\|) > 0 \tag{A.15}$$

and one of repulsion if

$$\mathscr{C}(\|\boldsymbol{r} - \boldsymbol{r}_o\|) < 0. \tag{A.16}$$

We remark that a central force field is always conservative, since $\nabla \times \boldsymbol{\Psi} = \mathbf{0}$. Now consider the specific choice

$$V = \underbrace{\frac{\alpha_1\|\boldsymbol{r} - \boldsymbol{r}_o\|^{\beta_1+1}}{\beta_1 + 1}}_{\text{attraction}} - \underbrace{\frac{\alpha_2\|\boldsymbol{r} - \boldsymbol{r}_o\|^{-\beta_2+1}}{-\beta_2 + 1}}_{\text{repulsion}}, \tag{A.17}$$

where all of the parameters, $\alpha$'s and $\beta$'s, are nonnegative. The gradient yields

$$-\nabla V = \boldsymbol{\Psi} = (\alpha_1\|\boldsymbol{r} - \boldsymbol{r}_o\|^{\beta_1} - \alpha_2\|\boldsymbol{r} - \boldsymbol{r}_o\|^{-\beta_2})\boldsymbol{n}, \tag{A.18}$$

which is repeatedly used later in this monograph. If a particle which is displaced slightly from an equilibrium point tends to return to that point, then we call that point a point of stability or stable point, and the equilibrium is said to be stable. Otherwise we say that the point is one of instability and the equilibrium is unstable. *A necessary and sufficient condition for a point of equilibrium to be stable is that the potential V at that point be a minimum.* The general condition by which a potential is stable for the multi-dimensional case can be determined by studying the properties of the Hessian of $V$,

$$[\mathbb{H}] \stackrel{\text{def}}{=} \begin{bmatrix} \frac{\partial^2 V}{\partial x_1 \partial x_1} & \frac{\partial^2 V}{\partial x_1 \partial x_2} & \frac{\partial^2 V}{\partial x_1 \partial x_3} \\ \frac{\partial^2 V}{\partial x_2 \partial x_1} & \frac{\partial^2 V}{\partial x_2 \partial x_2} & \frac{\partial^2 V}{\partial x_2 \partial x_3} \\ \frac{\partial^2 V}{\partial x_3 \partial x_1} & \frac{\partial^2 V}{\partial x_3 \partial x_2} & \frac{\partial^2 V}{\partial x_3 \partial x_3} \end{bmatrix}, \tag{A.19}$$

around an equilibrium point. A sufficient condition for $V$ to attain a minimum at an equilibrium point is for the Hessian be positive definite (which implies that $V$ is locally convex). For more details see Hale and Kocak [38].

**Remark 1.** Provided that the $\alpha$'s and $\beta$'s are selected appropriately, the chosen central force potential form is stable for motion in the normal direction, i.e. the line connecting the centers of particles in particle–particle interaction.[9] In order to determine stable parameter combinations, consider a potential function for a single particle, in one-dimensional motion, representing the motion in the normal direction, attracted and repulsed from a point $r_o$, measured by the coordinate $r$,

$$V = \frac{\alpha_1}{\beta_1 + 1}|r - r_o|^{\beta_1+1} - \frac{\alpha_2}{-\beta_2 + 1}|r - r_o|^{-\beta_2+1}, \tag{A.20}$$

whose derivative produces the form of interaction forces introduced earlier:

$$\Psi = -\frac{\partial V}{\partial r} = \left(\alpha_1|r - r_o|^{\beta_1} - \alpha_2|r - r_o|^{-\beta_2}\right)n, \tag{A.21}$$

where $n = \frac{r_o - r}{|r - r_o|}$. For stability, we require[10]

$$\frac{\partial^2 V}{\partial r^2} = \alpha_1\beta_1|r - r_o|^{\beta_1-1} + \alpha_2\beta_2|r - r_o|^{-\beta_2-1} > 0. \tag{A.23}$$

Thus, provided that the $\alpha$'s and $\beta$'s are all positive, then the potential form is stable. A static equilibrium point, $r = r_e$, can be calculated from $\Psi(|r_e - r_o|) = -\alpha_1|r_e - r_o|^{-\beta_1} + \alpha_2|r_e - r_o|^{-\beta_2} = 0$, which implies

$$|r_e - r_o| = \left(\frac{\alpha_2}{\alpha_1}\right)^{\frac{1}{\beta_1+\beta_2}}. \tag{A.24}$$

Inserting Eq. (A.24) into Eq. (A.23) yields a restriction for stability

$$\frac{\beta_2}{\beta_1} > -1, \tag{A.25}$$

which for the positive parameter selections ($\alpha$'s and $\beta$'s) is always satisfied. Thus, the central force potential in Eq. (A.17) is stable for motion in the normal direction, i.e. the line connecting the centers of the particles. For disturbances in directions orthogonal to the normal direction, the potential is neutrally stable, i.e. the Hessian's determinant is zero, thus indicating that the potential does not change for such perturbations.

**Remark 2.** In MD calculations, more complex potentials are often used, and typically take the form

$$V = \sum_{i,j} V_2 + \sum_{i,j,k} V_3 + \cdots \tag{A.26}$$

where $V_2$ is the binary, $V_3$ tertiary, etc. potential energy functions, and the summations are taken over corresponding combinations

[9] For disturbances in directions orthogonal to the normal direction, the potential is neutrally stable, i.e. the Hessian's determinant is zero, thus indicating that the potential does not change for such perturbations. The motion analysis of in the normal direction is relevant for central forces of the type under consideration.

[10] Note that

$$\frac{\partial^2 n}{\partial r^2} = 0. \tag{A.22}$$

of atoms. The binary functions usually take the form of the familiar Mie, Lennard-Jones, and Morse potentials [66]. The expansions beyond the binary interactions introduce either three-body terms directly [77] or as "local" modifications of the two-body terms [84]. Readers are referred to Frenklach and Carmer [28] for a survey of MD-type models, which includes comparisons of the theoretical and computational properties of a variety of interaction laws. The MD approach has been applied to description of solid, liquid, and gaseous phases, as well as biological systems (see Hase [39], Schlick [75] and Rapaport [74]).

### A.3. Stability interpretation

One can consider the convexity requirement on the potential to insure that the perturbed motion to a dynamical state remain small. Consider the dynamics of a particle in the normal direction, with a perturbation, $\tilde{r} = r + \delta r, m\ddot{\tilde{r}} = \Psi(\tilde{r})$, where $r$ is the perturbation-free position vector of the particle, governed by $m\ddot{r} = \Psi(r)$. Taking the difference between these two differential equations yields

$$m\ddot{\delta r} = \Psi(\tilde{r}) - \Psi(r) \approx \frac{\partial \Psi}{\partial r}|_{\tilde{r}=r}\delta r + \cdots \Rightarrow m\ddot{\delta r} - \frac{\partial \Psi}{\partial r}|_{\tilde{r}=r}\delta r \approx 0. \tag{A.27}$$

If $\frac{\partial \Psi(r)}{\partial r}$ is positive, there will be exponential growth of the perturbation, while if $\frac{\partial \Psi(r)}{\partial r}$ is negative, there will be oscillatory behavior of the perturbation. Thus, since $-\frac{\partial^2 V}{\partial r^2} = \frac{\partial \Psi}{\partial r}$, we have

$$m\ddot{\delta r} + \frac{\partial^2 V}{\partial r^2}|_{\tilde{r}=r}\delta r \approx 0. \tag{A.28}$$

The convexity of the potential simply corresponds to the positiveness of the stiffness at $r$.

## Appendix B. Basic properties of swarm-type models

The governing equations are formally similar to classical, normalized, linear (or linearized) second-order equations governing a one degree of freedom harmonic oscillator of the form

$$\ddot{r} + 2\zeta\omega_n\dot{r} + \omega_n^2 r = \frac{f(t)}{m}, \tag{B.1}$$

where $\omega_n = \sqrt{\frac{k}{m}}$, $r$ is the position measured from equilibrium ($r = 0$), $k$ is the stiffness associated with the restoring force $(kr)$, $m$ represents the mass, and where the damping ratio is $\zeta \stackrel{\text{def}}{=} \frac{d}{2m\omega_n}$, $d$ being a constant of damping and $f(t)$ is an external forcing term. The damped period of natural, *force-free*, vibration is $\mathscr{T}_d \stackrel{\text{def}}{=} \frac{2\pi}{\omega_d}$, where $\omega_d \stackrel{\text{def}}{=} \omega_n\sqrt{1-\zeta^2}$ is the "damped natural frequency". Using standard procedures, one decomposes the solution into homogeneous and particular parts, $r = r_H + r_P$. The homogeneous part must satisfy

$$\ddot{r}_H + 2\zeta\omega_n\dot{r}_H + \omega_n^2 r_H = 0. \tag{B.2}$$

Assuming the standard form $r_H = \exp(\lambda t)$, yields, upon substitution,

$$\lambda^2\exp(\lambda t) + 2\zeta\omega_n\lambda\exp(\lambda t) + \omega_n^2\exp(\lambda t) = 0, \tag{B.3}$$

leading to the characteristic equation

$$\lambda^2 + 2\zeta\omega_n\lambda + \omega_n^2 = 0. \tag{B.4}$$

Solving for the roots yields

$$\lambda_{1,2} = \omega_n\left(-\zeta \pm \sqrt{\zeta^2 - 1}\right). \tag{B.5}$$

The general solution is

$$r = A_1\exp(\lambda_1 t) + A_2\exp(\lambda_2 t). \tag{B.6}$$

Depending on the value of $\zeta$, the solution will have one of three distinct types of behavior:

- $\zeta > 1$, overdamped, leading to no oscillation, where the value of $r$ approaches zero for large values of time. Mathematically, $\lambda_1$ and $\lambda_2$ are negative numbers, thus

$$r_H = A_1\exp\left(\omega_n\left(-\zeta + \sqrt{\zeta^2-1}\right)t\right) + A_2 \times \exp\left(\omega_n\left(-\zeta - \sqrt{\zeta^2-1}\right)t\right). \tag{B.7}$$

- $\zeta = 1$, critically damped, leading to no oscillation, where the value of $r$ approaches zero for large values of time, however faster than the overdamped solution. Mathematically, $\lambda_1$ and $\lambda_2$ are equal real numbers, $\lambda_1 = \lambda_2 = -\omega_n$, thus

$$r_H = (A_1 + A_2 t)\exp(\omega_n t). \tag{B.8}$$

- $\zeta < 1$, underdamped, leading to damped oscillation, where the value of $r$ approaches zero for large values of time, in an oscillatory fashion. Mathematically, $\zeta^2 - 1 < 0$, thus

$$r_H = A_1\cos(\omega_d t) + A_2\sin(\omega_d t). \tag{B.9}$$

Thus, under certain conditions, a particulate flow can vibrate or "pulse". The particular solution, generated by the presence of externally applied forces, satisfies the differential equation for a specific righthand side

$$\ddot{r}_P + 2\zeta\omega_n\dot{r}_P + \omega_n^2 r_P = \frac{f(t)}{m}. \tag{B.10}$$

For example, if $f(t) = f_o\sin(\Omega t)$,

$$r_P = R\sin(\Omega t - \phi), \tag{B.11}$$

where

$$R = \frac{f_o}{k\sqrt{\left(1-\frac{\Omega^2}{\omega_n^2}\right)^2 + \left(2\zeta\frac{\Omega}{\omega_n}\right)^2}}, \tag{B.12}$$

and

$$\phi = \tan^{-1}\left(\frac{2\zeta\frac{\Omega}{\omega_n}}{1-\frac{\Omega^2}{\omega_n^2}}\right). \tag{B.13}$$

In order to qualitatively tie this directly to the form of problem considered in this work, consider a linearization of a single nonlinear differential equation, describing the attraction and repulsion from the origin ($r_o = 0$) of the form[11]

$$m\ddot{r} + d\dot{r} = \Psi(r), \tag{B.14}$$

where

$$\Psi(r) = -\alpha_1 r^{-\beta_1} + \alpha_2 r^{-\beta_2}, \tag{B.15}$$

and where $d$ is an effective dissipation term. Upon linearization of the nonlinear interaction relation about a point $r_*$,

$$\Psi(r) \approx \Psi(r_*) + \left.\frac{\partial \Psi}{\partial r}\right|_{r=r_*}(r - r_*) + \mathscr{O}(r - r_*), \tag{B.16}$$

and normalizing the equations, we obtain

$$\ddot{r} + 2\zeta^*\omega_n^*\dot{r} + (\omega_n^*)^2 r = \frac{f^*(t)}{m}, \tag{B.17}$$

where

$$\omega_n^* = \sqrt{\frac{-\left.\frac{\partial \Psi}{\partial r}\right|_{r=r_*}}{m}}, \tag{B.18}$$

[11] The unit normal has been taken into account, thus the presence of a change in sign.

where $\zeta^* = \frac{d}{2m\omega_n^*}$ and where

$$f^*(t) = \Psi(r_*) - \left.\frac{\partial \Psi}{\partial r}\right|_{r=r_*} r_*. \tag{B.19}$$

For the specific interaction form chosen we have

$$\omega_n^* = \sqrt{\frac{\alpha_1\beta_1 r_*^{\beta_1-1} + \alpha_2\beta_2 r_*^{-\beta_2-1}}{m}}, \tag{B.20}$$

and where the "loading" is

$$f^*(t) = \alpha_1 r_*^{\beta_1} + \alpha_2 r_*^{-\beta_2} + \alpha_1\beta_1 r_*^{\beta_1-1} + \alpha_2\beta_2 r_*^{-\beta_2-1}. \tag{B.21}$$

If $r_*$ is chosen as the static equilibrium point, $r_e$, then

$$r_* = r_e = \left(\frac{\alpha_2}{\alpha_1}\right)^{\frac{1}{\beta_1+\beta_2}} \tag{B.22}$$

and

$$\omega_n^* = \sqrt{\frac{1}{m}\left(\alpha_1\beta_1\left(\frac{\alpha_2}{\alpha_1}\right)^{\frac{\beta_1-1}{\beta_1+\beta_2}} + \alpha_2\beta_2\left(\frac{\alpha_2}{\alpha_1}\right)^{\frac{-\beta_2-1}{\beta_1+\beta_2}}\right)} \stackrel{\text{def}}{=} \sqrt{\frac{k^*}{m}}, \tag{B.23}$$

where

$$k^* \stackrel{\text{def}}{=} \left(\alpha_1\beta_1\left(\frac{\alpha_2}{\alpha_1}\right)^{\frac{\beta_1-1}{\beta_1+\beta_2}} + \alpha_2\beta_2\left(\frac{\alpha_2}{\alpha_1}\right)^{\frac{-\beta_2-1}{\beta_1+\beta_2}}\right). \tag{B.24}$$

Thus, if we kept the ratio $\frac{\alpha_1}{\alpha_2}$ constant, however increasing $\alpha_1$ (while keeping $m$ constant), we would effectively be increasing the "stiffness" in the system. Also, note that if $\alpha_2 = \beta_1 = \beta_2 = 0$, then this collapse to the familiar linear harmonic oscillator. Clearly, under certain conditions, a particulate flow may "pulse" (oscillate) depending on the character of the interaction and the contact parameters. Thus, oscillatory behavior is not unexpected for the multibody system. We remark that, increasingly smaller $\omega_n^*$ indicates that the system tends toward a "regular" non-interacting system. Smaller $\omega_n^*$ would occur with smaller attractive forces, and larger values of $\zeta^*$ (more damped). Clearly, key dimensionless parameters, like $\zeta^*$, characterize the oscillatory behavior and the fluctuating motion with respect to mean values within the swarm.

## Appendix C. A genetic algorithm

Here we summarize a genetic algorithm found in Zohdi [87–93] which has been developed to treat nonconvex inverse problems involving multi-particle systems. The central idea is that the system parameters form a genetic string and a survival of the fittest algorithm is applied to a population of such strings. The overall process is: (a) a population ($S$) of different parameter sets are generated at random within the parameter space, each represented by a ("genetic") string of the system ($N$) parameters, (b) the performance of each parameter set is tested, (c) the parameter sets are ranked from top to bottom according to their performance, (d) the best parameter sets (parents) are mated pairwise producing two offspring (children), i.e. each best pair exchanges information by taking random convex combinations of the parameter set components of the parents' genetic strings and (e) the worst performing genetic strings are eliminated, new replacement parameter sets (genetic strings) are introduced into the remaining population of best performing genetic strings and the process (a–e) is then repeated. The term "fitness" of a genetic string is used to indicate the value of the objective function. The most fit genetic string is the one with the smallest objective function. The retention of the top fit genetic strings from a previous generation (parents) is critical, since if the objective functions are highly nonconvex (the present case), there exists a clear possibility that the inferior offspring will replace superior parents. When the top parents are retained, the minimization of the cost function is guaranteed to be monotone (guaranteed improvement) with increasing generations. There is no guarantee of successive improvement if the top parents are not retained, even though nonretention of parents allows more new genetic strings to be evaluated in the next generation. In the scientific literature, numerical studies imply that, for sufficiently large populations, the benefits of parent retention outweigh this advantage and any disadvantages of "inbreeding", i.e. a stagnant population. For more details on this so-called "inheritance property" see Davis [17] or Kennedy and Eberhart [59]. In the upcoming algorithm, inbreeding is mitigated since, with each new generation, new parameter sets, selected at random within the parameter space, are added to the population. Previous numerical studies of the author [87–93] have indicated that not retaining the parents is suboptimal due to the possibility that inferior offspring will replace superior parents. Additionally, parent retention is computationally less expensive, since these parameter sets do not have to be reevaluated (on ranked) in the next generation. An implementation of such ideas is as follows [87–93]:

- **Step 1**: Randomly generate a population of $S$ starting genetic strings, $\boldsymbol{\Lambda}^i, (i = 1, \ldots, S) : \boldsymbol{\Lambda}^i \stackrel{\text{def}}{=} \{\Lambda_1^i, \Lambda_2^i, \Lambda_3^i, \Lambda_4^i, \ldots, \ldots \Lambda_N^i\} = \{\alpha_1^i, \beta_1^i, \alpha_2^i, \beta_2^i, \ldots\}$.
- **Step 2**: Compute fitness of each string $\Pi(\boldsymbol{\Lambda}^i), (i = 1, \ldots, S)$.
- **Step 3**: Rank genetic strings: $\boldsymbol{\Lambda}^i, (i = 1, \ldots, S)$.
- **Step 4**: Mate nearest pairs and produce two offspring, $(i = 1, \ldots, S)\boldsymbol{\lambda}^i \stackrel{\text{def}}{=} \Phi^{(I)}\boldsymbol{\Lambda}^i + (1 - \Phi^{(I)})\boldsymbol{\Lambda}^{i+1}, \boldsymbol{\lambda}^{i+1} \stackrel{\text{def}}{=} \Phi^{(II)}\boldsymbol{\Lambda}^i + (1 - \Phi^{(II)})\boldsymbol{\Lambda}^{i+1}$.
- **Note**: $\Phi^{(I)}$ and $\Phi^{(II)}$ are random numbers, such that $0 \leqslant \Phi^{(I)}, \Phi^{(II)} \leqslant 1$, which are different for each component of each genetic string.
- **Step 5**: Kill off bottom $M < S$ strings and keep top $K < N$ parents and top $K$ offspring ($K$ offspring + $K$ parents + $M$ = $S$).
- **Step 6**: Repeat Steps 1–6 with top gene pool ($K$ offspring and $K$ parents), plus $M$ new, randomly generated, strings.
- **Option**: Rescale and restart search around best performing parameter set every few generations.
- **Option**: We remark that gradient-based methods are sometimes useful for post-processing solutions found with a genetic algorithm, if the objective function is sufficiently smooth in that region of the parameter space. In other words, if one has located convex portion of the parameter space with a global genetic search, one can employ gradient-based procedures locally to minimize the objective function further. In such procedures, in order to obtain a new directional step for $\boldsymbol{\Lambda}$, one must solve the following system:

$$[\mathbb{H}]\{\Delta\boldsymbol{\Lambda}\} = -\{\boldsymbol{g}\}, \tag{C.1}$$

where $[\mathbb{H}]$ is the Hessian matrix $(N \times N)$, where $\{\Delta\boldsymbol{\Lambda}\}$ is the parameter increment $(N \times 1)$, and $\{\boldsymbol{g}\}$ is the gradient $(N \times 1)$. Extensive reviews of these methods can be found in Luenberger [65], Gill et al. [30] and Papadrakakis et al. [73].

## References


[1] W.F. Ames, Numerical Methods for Partial Differential Equations, second ed., Academic Press, 1977.
[2] O. Axelsson, Iterative Solution Methods, Cambridge University Press, 1994.
[3] M. Ballerini, N. Cabibbo, R. Candelier, A. Cavagna, E. Cisbani, I. Giardina, V. Lecomte, A. Orlandi, G. Parisi, A. Procaccini, M. Viale, V. Zdravkovic, Interaction ruling animal collective behavior depends on topological rather than metric distance: evidence from a field study, PNAS 105 (4) (2008) 1232–1237.
[4] R.P. Behringer, G.W. Baxter, Pattern formation, complexity & time-dependence in granular flows, in: A. Mehta (Ed.), Granular Matter – An Interdisciplinary Approach, Springer-Verlag, New York, 1993, pp. 85–119.
[5] R.P. Behringer, The dynamics of flowing sand, Nonlinear Sci. Today 3 (1993) 1.
[6] R.P. Behringer, B.J. Miller, Stress fluctuations for sheared 3D granular materials, in: R. Behringer, J. Jenkins (Eds.), Proceedings, Powders & Grains, vol. 97, Balkema, 1997, pp. 333–336.

[7] R.P. Behringer, D. Howell, C. Veje, Fluctuations in granular flows, Chaos 9 (1999) 559–572.
[8] J. Bender, R. Fenton, On the flow capacity of automated highways, Transport Sci. 4 (February) (1970) 52–63.
[9] G. Beni, The concept of cellular robotic system, in: IEEE International Symposium on Intelligent Control, 1988, pp. 57–62.
[10] Y.A. Berezin, K. Hutter, L.A. Spodareva, Stability properties of shallow granular flows, Int. J. NonLinear Mech. 33 4 (1998) 647–658.
[11] E. Bonabeau, M. Dorigo, G. Theraulaz, Swarm Intelligence: From Natural to Artificial Systems, Oxford University Press, New York, 1999.
[12] E. Bonabeau, M. Dorigo, G. Theraulaz, Swarm Intelligence: From Natural to Artificial Systems, Oxford University Press, New York, 1999. pp. 57–62.
[13] E. Bonabeau, C. Meyer, Swarm intelligence: a whole new way to think about business, Harvard Business Rev. 79 (5) (2001) 106–114.
[14] C.M. Breder, Equations descriptive of fish schools and other animal aggregations, Ecology 35 (3) (1954) 361–370.
[15] R.A. Brooks, Intelligence without reason, in: Proceedings of the International Joint Conference on Artificial Intelligence (IJCAI-91), 1991, pp. 569–595.
[16] Y.U. Cao, A.S. Fukunaga, A. Kahng, Cooperative mobile robotics: antecedents and directions, Auton. Robots 4 (1) (1997) 7–27.
[17] L. Davis, Handbook of Genetic Algorithms, Thompson Computer Press, 1991.
[18] A. Donev, I. Cisse, D. Sachs, E.A. Variano, F. Stillinger, R. Connelly, S. Torquato, P. Chaikin, Improving the density of jammed disordered packings using ellipsoids, Science 303 (13) (2004) 990–993.
[19] A. Donev, F.H. Stillinger, P.M. Chaikin, S. Torquato, Unusually dense crystal ellipsoid packings, Phys. Rev. Lett. 92 (2004) 255506.
[20] A. Donev, S. Torquato, F. Stillinger, Neighbor list collision-driven molecular dynamics simulation for nonspherical hard particles – I. Algorithmic details, J. Comput. Phys. 202 (2005) 737.
[21] A. Donev, S. Torquato, F. Stillinger, Neighbor list collision-driven molecular dynamics simulation for nonspherical hard particles – II. Application to ellipses and ellipsoids, J. Comput. Phys. 202 (2005) 765.
[22] A. Donev, S. Torquato, F.H. Stillinger, Pair correlation function characteristics of nearly jammed disordered and ordered hard-sphere packings, Phys. Rev. E 71 (2005) 011105.
[23] G. Dudek, M. Jenkin, E. Milios, D. Wilkes, A taxonomy for multi-agent robotics, Auton. Robots 3 (1996) 375–397.
[24] M. Dorigo, V. Maniezzo, A. Colorni, Ant system: optimization by a colony of cooperating agents, IEEE Trans. Systems Man Cybernet. B 26 (1) (1996) 29–41.
[25] J. Duran, Sands, Powders and Grains, An Introduction to the Physics of Granular Matter, Springer-Verlag, 1997.
[26] T. Feder, Statistical Physics is for the Birds, Phys. Today (2007) 28–29.
[27] E. Fiorelli, N.E. Leonard, P. Bhatta, D. Paley, R. Bachmayer, D.M. Fratantoni, Multi-auv control and adaptive sampling in monterey bay, in: Autonomous Underwater Vehicles, 2004 IEEE/OES, 2004, pp. 134–147.
[28] M. Frenklach, C.S. Carmer, Molecular dynamics using combined quantum & empirical forces: application to surface reactions, In: Advances in Classical Trajectory Methods, vol. 4, 1999, pp. 27–63.
[29] V. Gazi, K.M. Passino, Stability analysis of swarms, in: Proceedings of the American Control Conference. Anchorage, AK, May 8–10, 2002.
[30] P. Gill, W. Murray, M. Wright, Practical Optimization, Academic Press, 1995.
[31] D.E. Goldberg, Genetic Algorithms in Search, Optimization & Machine Learning, Addison-Wesley, 1989.
[32] D.E. Goldberg, K. Deb, Special issue on genetic algorithms, Comput. Methods Appl. Mech. Engrg. 186 (2-4) (2000) 121–124.
[33] J.M.N.T. Gray, M. Wieland, K. Hutter, Gravity-driven free surface flow of granular avalanches over complex basal topography, Proc. Roy. Soc. Lond. A 455 (1999) 1841–1874.
[34] J.M.N.T. Gray, K. Hutter, Pattern formation in granular avalanches, Continuum Mech. Thermodyn. 9 (1997) 341–345.
[35] J.M.N.T. Gray, Granular flow in partially filled slowly rotating drums, J. Fluid Mech. 441 (2001) 1–29.
[36] R. Greve, K. Hutter, Motion of a granular avalanche in a convex & concave curved chute: experiments & theoretical predictions, Philos. Trans. Roy. Soc. Lond. A 342 (1993) 573–600.
[37] J.M. Haile, Molecular Dynamics Simulations: Elementary Methods, Wiley, 1992.
[38] J. Hale, H. Kocak, Dynamics & Bifurcations, Springer-Verlag, 1991.
[39] W.L. Hase, Molecular dynamics of clusters, surfaces, liquids, & interfaces, Advances in Classical Trajectory Methods, vol. 4, JAI Press, 1999.
[40] J.K. Hedrick, D. Swaroop, Dynamic coupling in vehicles under automatic control, in: 13th IAVSD Symposium, August 1993, pp. 209–220.
[41] J.K. Hedrick, M. Tomizuka, P. Varaiya, Control issues in automated highway systems, IEEE Contr. Syst. Mag. 14 (6) (1994) 21–32.
[42] J.H. Holland, Adaptation in Natural & Artificial Systems, University of Michigan Press, Ann Arbor, Mich, 1975.
[43] K. Hutter, Avalanche dynamics, in: V.P. Singh (Ed.), Hydrology of Disasters, Kluwer Academic Publishers, Dordrecht, 1996, pp. 317–394.
[44] K. Hutter, T. Koch, C. Plüss, S.B. Savage, The dynamics of avalanches of granular materials from initiation to runout. Part II. Experiments, Acta Mech. 109 (1995) 127–165.
[45] K. Hutter, K.R. Rajagopal, On flows of granular materials, Continuum Mech. Thermodyn. 6 (1994) 81–139.
[46] K. Hutter, M. Siegel, S.B. Savage, Y. Nohguchi, Two-dimensional spreading of a granular avalanche down an inclined plane. Part I: theory, Acta Mech. 100 (1993) 37–68.
[47] H.M. Jaeger, S.R. Nagel, La Physique de l'Etat Granulaire, La Recherche 249 (1992) 1380.
[48] H.M. Jaeger, S.R. Nagel, Physics of the granular state, Science 255 (1992) 1523.
[49] H.M. Jaeger, S.R. Nagel, La Fisica del Estado Granular, Mundo Cientifico 132 (1993) 108.
[50] H.M. Jaeger, J.B. Knight, C.H. Liu, S.R. Nagel, What is shaking in the sand box?, Mat Res. Soc. Bull. 19 (1994) 25.
[51] H.M. Jaeger, S.R. Nagel, R.P. Behringer, The physics of granular materials, Phys. Today 4 (1996) 32.
[52] H.M. Jaeger, S.R. Nagel, R.P. Behringer, Granular solids, liquids & gases, Rev. Mod. Phys. 68 (1996) 1259.
[53] H.M. Jaeger, S.R. Nagel, Dynamics of granular material, Am. Sci. 85 (1997) 540.
[54] J.T. Jenkins, O.D.L. Strack, Mean-field inelastic behavior of random arrays of identical spheres, Mech. Mater. 16 (1993) 25–33.
[55] J.T. Jenkins, L. La Ragione, Particle spin in anisotropic granular materials, Int. J. Solids Struct. 38 (1999) 1063–1069.
[56] J.T. Jenkins, M.A. Koenders, The incremental response of random aggregates of identical round particles, Eur. Phys. J. E-Soft Mat. 13 (2004) 113–123.
[57] J.T. Jenkins, D. Johnson, L. La Ragione, H. Makse, Fluctuations and the effective moduli of an isotropic, random aggregate of identical, frictionless spheres, J. Mech. Phys. Solids 53 (2005) 197–225.
[58] A. Kansaal, S. Torquato, F. Stillinger, Diversity of order and densities in jammed hard-particle packings, Phys. Rev. E 66 (2002) 041109.
[59] J. Kennedy, R. Eberhart, Swarm Intelligence, Morgan Kaufmann Publishers, 2001.
[60] T. Koch, R. Greve, K. Hutter, Unconfined flow of granular avalanches along a partly curved surface. II. Experiments & numerical computations, Proc. Roy. Soc. Lond. A 445 (1994) 415–435.
[61] N. Lagaros, M. Papadrakakis, G. Kokossalakis, Structural optimization using evolutionary algorithms, Comput. Struct. 80 (2002) 571–589.
[62] C.H. Liu, H.M. Jaeger, S.R. Nagel, Finite size effects in a sandpile, Phys. Rev. A 43 (1991) 7091.
[63] C.H. Liu, S.R. Nagel, Sound in a granular material: disorder & nonlinearity, Phys. Rev. B 48 (1993) 15646.
[64] Liu Yang, M. Passino Kevin, Swarm intelligence: literature overview. Technical report, Ohio State University, March 2000.
[65] D. Luenberger, Introduction to Linear & Nonlinear Programming, Addison-Wesley, Menlo Park, 1974.
[66] E.A. Moelwyn-Hughes, Physical Chemistry, Pergamon, 1961.
[67] S.R. Nagel, Instabilities in a sandpile, Rev. Mod. Phys. 64 (1992) 321.
[68] C. Onwubiko, Introduction to Engineering Design Optimization, Prentice Hall, 2000.
[69] M. Papadrakakis, N. Lagaros, G. Thierauf, J. Cai, Advanced solution methods in structural optimisation using evolution strategies, Engrg. Comput. J. 15 (1) (1998) 12–34.
[70] M. Papadrakakis, N. Lagaros, Y. Tsompanakis, Structural optimization using evolution strategies and neutral networks, Comput. Methods Appl. Mech. Engrg. 156 (1) (1998) 309–335.
[71] M. Papadrakakis, N. Lagaros, Y. Tsompanakis, Optimization of large-scale 3D trusses using evolution strategies and neural networks, Int. J. Space Struct. 14 (3) (1999) 211–223.
[72] M. Papadrakakis, J. Tsompanakis, N. Lagaros, Structural shape optimisation using evolution strategies, Engrg. Optim. 31 (1999) 515–540.
[73] M. Papadrakakis, N. Lagaros, Y. Tsompanakis, V. Plevris, Large scale structural optimization: computational methods and optimization algorithms, Arch. Comput. Methods Engrg. State of the art Rev. 8 (3) (2001) 239–301.
[74] D.C. Rapaport, The Art of Molecular Dynamics Simulation, Cambridge University Press, 1995.
[75] T. Schlick, Molecular Modeling & Simulation. An Interdisciplinary Guide, Springer-Verlag, New York, 2000.
[76] J.S. Shamma, A connection between structured uncertainty and decentralized control of spatially invariant systems, in: Proceedings of the 2001 American Control Conference, Arlington, VA, Part 4, 2001, pp. 3117–3121.
[77] F.H. Stillinger, T.A. Weber, Computer simulation of local order in condensed phases of silicon, Phys. Rev. B 31 (1985) 5262–5271.
[78] D. Swaroop, J.K. Hedrick, String stability of interconnected systems, IEEE Trans. Automat. Contr. 41 (4) (1996) 349–356.
[79] D. Swaroop, J.K. Hedrick, Constant spacing strategies for platooning in automated highway systems, J. Dyn. Syst. Measure. Contr. September (1999) 462–470.
[80] Y.C. Tai, S. Noelle, J.M.N.T. Gray, K. Hutter, Shock capturing & front tracking methods for granular avalanches, J. Comput. Phys. 175 (2002) 269–301.
[81] Y.C. Tai, J.M.N.T. Gray, K. Hutter, S. Noelle, Flow of dense avalanches past obstructions, Annals of Glaciology 32 (2001) 281–284.
[82] Y.C. Tai, S. Noelle, J.M.N.T. Gray, K. Hutter, An accurate shock-capturing finite-difference method to solve the Savage-Hutter equations in avalanche dynamics, Ann. Glaciol. 32 (2001) 263–267.
[83] S. Torquato, Random Heterogeneous Materials: Microstructure and Macroscopic Properties, Springer-Verlag, New York, 2002.
[84] J. Tersoff, Empirical interatomic potential for carbon, with applications to amorphous carbon, Phys. Rev. Lett. 61 (1988) 2879–2882.
[85] M. Wieland, J.M.N.T. Gray, K. Hutter, Channelized free-surface flow of cohesionless granular avalanches in a chute with shallow lateral curvature, J. Fluid Mech. 392 (1999) 73–100.

[86] T.I. Zohdi, An adaptive–recursive staggering strategy for simulating multifield coupled processes in microheterogeneous solids, Int. J. Numer. Methods Engrg. 53 (2002) 1511–1532.
[87] T.I. Zohdi, Computational design of swarms, Int. J. Numer. Methods Engrg. 57 (2003) 2205–2219.
[88] T.I. Zohdi, Modeling and simulation of a class of coupled thermo-chemo-mechanical processes in multiphase solids, Comput. Methods Appl. Mech. Engrg. 193 (6-8) (2004) 679–699.
[89] T.I. Zohdi, Genetic optimization of statistically uncertain microheterogeneous solids, Philos. Trans. Roy. Soc.: Math. Phys. Engrg. Sci. 361 (1806) (2003) 1021–1043.
[90] T.I. Zohdi, Modeling and direct simulation of near-field granular flows, Int. J. Solids Struct. 42 (2) (2004) 539–564.
[91] T.I. Zohdi, A computational framework for agglomeration in thermo-chemically reacting granular flows, Proc. Roy. Soc. 460 (2052) (2004) 3421–3445.
[92] T.I. Zohdi, Constrained inverse formulations in random material design, Comput. Methods Appl. Mech. Engrg. 192 (28–30, 18) (2003) 3179–3194.
[93] T.I. Zohdi, P. Wriggers, Introduction to Computational Micromechanics, Springer-Verlag, 2005.
[94] T.I. Zohdi, Charge-induced clustering in multifield granular flow, Int. J. Numer. Methods Engrg. 62 (7) (2005) 870–898.
[95] T.I. Zohdi, Computation of strongly coupled multifield interaction in particle-fluid systems, Comput. Methods Appl. Mech. Engrg. 196 (2007) 3927–3950.
[96] T.I. Zohdi, Particle collision and adhesion under the influence of near-fields, J. Mech. Mater. Struct. 6 (2007) 1011–1018.
[97] T.I. Zohdi, Introduction to the modeling and simulation of particulate flows, SIAM (Society for Industrial and Applied Mathematics) (2007).